



## Studies on the variability of the Greenland Ice Sheet and climate

Kumiko Goto-Azuma<sup>a,b,\*</sup>, Tomoyuki Homma<sup>c</sup>, Tomotaka Saruya<sup>c,1</sup>, Fumio Nakazawa<sup>a,b</sup>,  
Yuki Komuro<sup>a</sup>, Naoko Nagatsuka<sup>a</sup>, Motohiro Hirabayashi<sup>a</sup>, Yutaka Kondo<sup>a</sup>, Makoto Koike<sup>d</sup>,  
Teruo Aoki<sup>a,b</sup>, Ralf Greve<sup>e,f</sup>, Jun'ichi Okuno<sup>a,b</sup>

<sup>a</sup> National Institute of Polar Research, 10-3 Midori-cho, Tachikawa, Tokyo, 190-8518, Japan

<sup>b</sup> The Graduate University for Advanced Studies, SOKENDAI, Shonan Village, Hayama, Kanagawa 240-0193, Japan

<sup>c</sup> Nagaoka University of Technology, Nagaoka, Niigata, 940-2188, Japan

<sup>d</sup> University of Tokyo, Department of Earth and Planetary Science, Graduate School of Science, The University of Tokyo, Hongo 7-3-1, Bunkyo-ku, Tokyo, 113-0033, Japan

<sup>e</sup> Institute of Low Temperature Science, Hokkaido University, Sapporo, 060-0819, Japan

<sup>f</sup> Arctic Research Center, Hokkaido University, Sapporo, 001-0021, Japan

### ARTICLE INFO

#### Keywords:

Greenland Ice Sheet  
Ice core  
Surface mass balance  
Flow law  
Sea level change

### ABSTRACT

We review major scientific results from Subtheme (1) "Variability of the Greenland Ice Sheet and climate" under Research Theme 2 "Variations in the ice sheet, glaciers, and the environment in the Greenland region" of the Arctic Challenge for Sustainability (ArCS) project. We participated in the international East Greenland Ice Core Project (EGRIP) led by Denmark, conducted snow pit observations near the coring site and reconstructed the surface mass balance over the past 10 years. Analyses of an ice core from Northwest Greenland revealed temporal variability in black carbon concentration over the past 350 years and in mineral dust over the past 100 years. To understand the mechanisms of ice-sheet flow, which is necessary for accurate predictions of sea level rise, we conducted laboratory experiments using artificial ice and derived an improved flow law for ice containing impurities. Ice sheet modeling was improved by including effects of impurities and ice stream dynamics. As part of the Ice Sheet Model Intercomparison Project for the Coupled Model Intercomparison Project Phase 6 (ISMIP6), we simulated ice sheet mass loss and contribution to sea level rise over the 21st century and beyond. Furthermore, we developed a Glacial Isostatic Adjustment model to better constrain ice sheet models.

### 1. Introduction

The Greenland Ice Sheet and the glaciers, ocean, climate and environment in and around Greenland have been experiencing drastic changes (e.g. AMAP, 2017), and have attracted international attention. However, the mechanisms underlying these changes and their impacts on the climate and the ocean are poorly understood. Changes in the coastal regions of Greenland have also been affecting local communities and their culture, but much is yet to be understood. Under these circumstances, we carried out studies under Research Theme 2—Variations in the ice sheet, glaciers, and environment in the Greenland region—of the Arctic Challenge for Sustainability (ArCS) project Subtheme (1) "Variability of the Greenland Ice Sheet and climate" with focus on interior Greenland and Subtheme (2) "Ice sheet/glacier–ocean interaction in Greenland" with focus on the coastal regions of Greenland. In this

paper, we introduce the background and purpose of Subtheme (1) and review its major scientific results. A paper by Sugiyama et al. (submitted to this issue) reviews the results from Subtheme (2).

Mass loss of the Greenland Ice Sheet has been accelerating (AMAP, 2017; IPCC, 2013) owing to global warming and associated environmental changes in the Arctic, which leads to sea level rise, and possibly abrupt changes in the global climate and ocean circulation. While the ice sheet was in a state of near balance in the early 1990s, the mass loss amounted to  $255 \pm 20$  Gt/yr ( $0.71 \pm 0.056$  mm/yr sea-level equivalent) between 2005 and 2015 (The IMBIE Team, 2020). These changes would influence human societies and economies, including those in Japan. A better understanding of the mechanisms and impacts of ice sheet mass loss and ongoing environmental changes from global warming is therefore crucial. There is also an urgent need to improve future projections of ice mass loss, sea level change, and environmental changes to

\* Corresponding author. National Institute of Polar Research, 10-3 Midori-cho, Tachikawa, Tokyo, 190-8518, Japan.

E-mail address: [kumiko@nipr.ac.jp](mailto:kumiko@nipr.ac.jp) (K. Goto-Azuma).

<sup>1</sup> Present address: National Institute of Polar Research, 10-3 Midori-cho, Tachikawa, Tokyo 190-8518, Japan.

<https://doi.org/10.1016/j.polar.2020.100557>

Received 25 March 2020; Received in revised form 28 June 2020; Accepted 6 July 2020

Available online 7 August 2020

1873-9652/© 2020 Elsevier B.V. and NIPR. All rights reserved.

prepare for such changes. Accelerated mass loss can be attributed to decreases in the surface mass balance of the ice sheet and increased ice flow into the ocean (Van den Broeke et al., 2009; Rignot et al., 2011). However, changes in surface mass balance, ice flow dynamics, and the environment associated with global warming remain poorly understood.

The major objectives of Subtheme (1) are to: (a) understand temporal and spatial variability in surface mass balance and its relationship with warming; (b) improve the flow law of ice sheet ice for future improvements of ice sheet models; (c) improve ice sheet and glacial isostatic adjustment (GIA) modeling for better projections of sea level change; and (d) reconstruct past environmental changes associated with warming to better understand the impacts of warming. We participated in the East Greenland Ice Core Project (EGRIP) in collaboration with Denmark, USA, Germany, Norway, France, Switzerland, and other countries. Under this international ice coring project, drilling of a deep ice core at the onset of the Northeast Greenland Ice Stream (NEGIS) to the bed of the ice sheet is underway, and various observations have been carried out (Fahnestock et al., 1993, 2001; Joughin et al., 2001). Horizontal flow velocity at this location is several tens of meters per year, which is much larger than that at previous deep ice coring sites (Joughin et al., 2001; Vallelonga et al., 2014). One of the main purposes of the EGRIP is to advance our knowledge on the dynamics and past changes of the Greenland Ice Sheet through analyses of the EGRIP core, ice-sheet and borehole observations and modeling studies. This is closely related to objectives (b) and (c). To accomplish objective (c), we must also realize objective (a). Another main purpose of EGRIP is to reconstruct the climate and environment during the early Holocene, which was warmer than today and serves as an excellent analogue for future conditions under global warming. This is closely related to objective (d). Participation in EGRIP also contributes to important goals of the ArCS project, which include the promotion of international collaborative research, establishment of research and observation stations in the Arctic, and dispatch of young researchers to Arctic research institutions.

We performed snow pit studies at the EGRIP site (Fig. 1) to understand recent variability in surface mass balance, which is one of the two major factors that affect ice sheet mass loss (objective (a), Section 2). The other major factor is ice flow dynamics. Therefore, we carried out creep tests of ice and derived an improved ice flow law to better understand ice flow properties and dynamics (objective (b), Section 3). At the EGRIP site, we participated in analyses of the physical properties of the EGRIP core and studied ice flow dynamics of the NEGIS. To evaluate the contribution of mass loss of the Greenland Ice Sheet to global sea level rise (objective (c), Section 4), we performed ice-sheet modeling studies, mainly as part of the Ice Sheet Model Intercomparison Project for the Coupled Model Intercomparison Project Phase 6 (CMIP6) (ISMIP6; Nowicki et al., 2020). Furthermore, we developed a GIA model, which is essential for constraining ice-sheet models (objective (c), Section 4). We also analyzed EGRIP and previous Greenland ice cores to study the impacts of past warmings (objective (d), Section 5). Our ultimate goal is to incorporate the achievements from objectives (a) and (b) and results from the GIA modeling into ice sheet models to better understand the interactions between ice sheets, climate, and the environment. As a first step, we carried out four individual projects to achieve objectives (a) - (d) during the 5-year ArCS project, as described in Sections 2-5. We have not yet used the results from Sections 2 - 3 for the ice sheet modeling described in Section 4. Nor have we linked the results from Sections 4 and 5 yet. These tasks remain for future studies.

## 2. Recent variability in surface mass balance at EGRIP

To investigate recent variability in surface mass balance in East Greenland, where direct observations are scarce, we carried out snow pit studies around the EGRIP drill site during the summers of 2016–2019. Using snow samples collected from snow-pit walls, we reconstructed recent surface mass balance and examined its spatial variability. It is important to examine the spatial variability and representativity of the

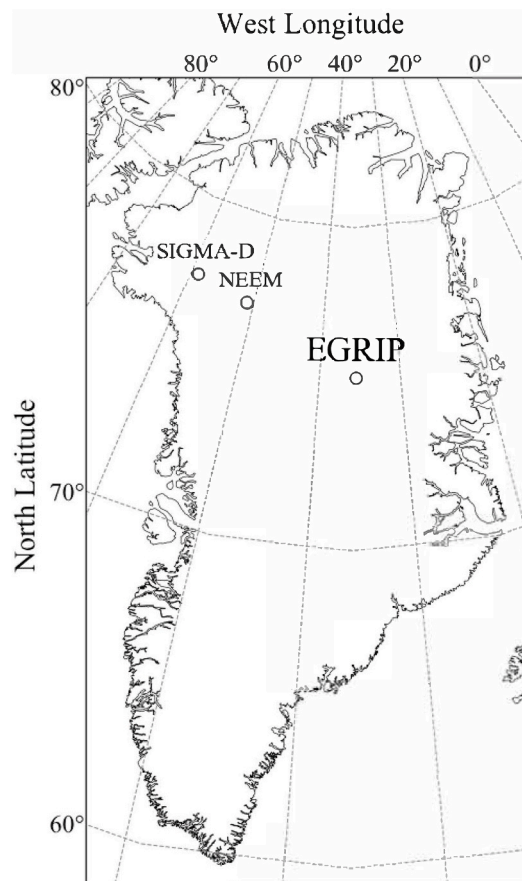


Fig. 1. Locations of ice coring sites in Greenland.

snow-pit data to discuss temporal variability around the EGRIP drill site. Although we reconstructed surface mass balances only around the EGRIP drill site, the results serve as ground truth data for satellite observations and can hence be extended to wider areas in Greenland. Results of the snow pit studies in 2016 are reported by Nakazawa et al. (submitted to this special issue) and those in 2017–2018 are reported by Komuro et al. (2020). Here, we summarize the results of all the snow pit studies.

Characteristics of the snow pits reported in Nakazawa et al. (submitted) and Komuro et al. (2020) are shown in Tables 1 and 2 and Fig. 2. Snow samples for stable water isotope and ion measurements were collected from each pit at depth intervals of 0.03 m. Samples for density measurements were also collected at the same depths from each pit and then weighed. Fig. 3 shows vertical profiles of stratigraphy,  $\delta^{18}\text{O}$ ,  $\delta\text{D}$ , d-excess (derived from  $\delta\text{D} - 8 \times \delta^{18}\text{O}$ ), methanesulfonate (hereafter referred to as MSA) and density in Pit 1. All profiles show clear seasonal variations. Because  $\delta^{18}\text{O}$  and  $\delta\text{D}$  peak in summer (e.g. Johnsen et al., 1989; Kuramoto et al., 2011), we determined summer layers using annual peaks of  $\delta^{18}\text{O}$  and  $\delta\text{D}$ . Because d-excess peaks in fall (e.g. Johnsen et al., 1989; Kuramoto et al., 2011) and MSA peaks in summer (Li et al., 1993; Jaffrezo et al., 1994; Kuramoto et al., 2011), annual peaks of d-excess and MSA were used as secondary tools for dating. Pit 2 was similarly dated using  $\delta^{18}\text{O}$ ,  $\delta\text{D}$ , d-excess and MSA (Nakazawa et al., submitted). Pits 3–6 were dated using  $\delta^{18}\text{O}$ ,  $\delta\text{D}$ , and d-excess (Komuro et al., 2020).

Although the annual layer of 2012–13 was particularly thin in Pit 1, that in Pit 2 had a regular thickness compared to other years (Nakazawa et al., submitted). The between-site difference of annual layer thickness can potentially be explained by spatial variability, as discussed by Komuro et al. (2020). In Pit 1, ice layers were observed at depths of 1.76 and 2.02 m (Fig. 3). The ice layers provide evidence of slight summer

**Table 1**

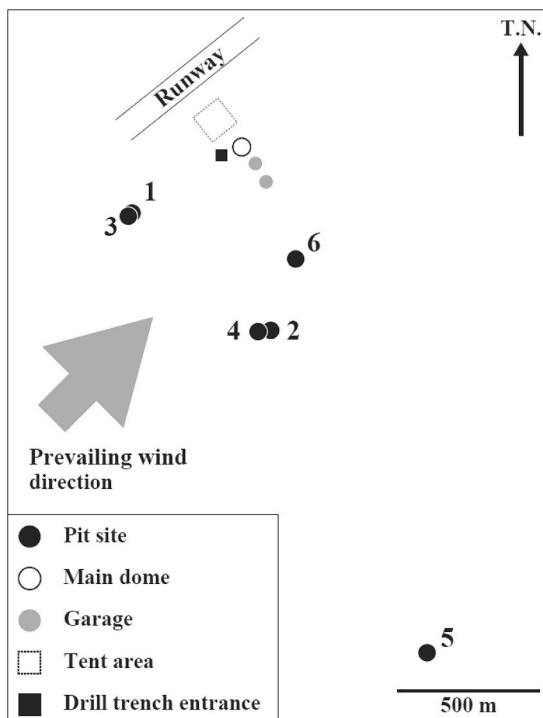
Characteristics of snow pits and average surface mass balance reconstructed from each pit for the period covered by each pit (Komuro et al., 2020).

	Observation date	Depth	Period covered	Longitude	Latitude	Average surface mass balance (mm w.e./yr)
Pit 1	2016/6/29–2016/7/5	4.02 m	2006–2016	75.6289°N	36.0039°W	145 ± 44
Pit 2	2016/7/11–2016/7/12	3.18 m	2009–2016	75.6252°N	35.9860°W	149 ± 23
Pit 3	2017/6/13	2.01 m	2013–2017	75.6288°N	36.0045°W	148 ± 17
Pit 4	2017/6/16	2.01 m	2013–2017	75.6252°N	35.9876°W	157 ± 19
Pit 5	2017/8/6–2017/8/8	2.22 m	2012–2017	75.6150°N	35.9658°W	144 ± 28
Pit 6	2018/7/3–2018/7/5	2.01 m	2014–2018	75.6275°N	35.9828°W	154 ± 16

**Table 2**

Seasonal snow depositions (mm water equivalent) for Pits 1 and 2. The average summer-to-winter and winter-to-summer depositions for the period covered by each pit are shown in the bottom row. SD indicates standard deviation (Komuro et al., 2020).

Period	Pit 1	Pit 2
Winter 2015/16 to summer 2016	70	82
Summer 2015 to winter 2015/16	72	58
Winter 2014/15 to summer 2015	73	50
Summer 2014 to winter 2014/15	95	100
Winter 2013/14 to summer 2014	59	86
Summer 2013 to winter 2013/14	89	102
Winter 2012/13 to summer 2013	29	60
Summer 2012 to winter 2012/13	29	72
Winter 2011/12 to summer 2012	90	66
Summer 2011 to winter 2011/12	111	107
Winter 2010/11 to summer 2011	70	42
Summer 2010 to winter 2010/11	88	95
Winter 2009/10 to summer 2010	79	91
Summer 2009 to winter 2009/10	64	35
Average of summer-to-winter depositions ±SD	78 ± 27	81 ± 27
Average of winter-to-summer depositions ±SD	67 ± 19	68 ± 19

**Fig. 2.** Locations of snow pit observation sites. Locations of Main Dome (main building located at 75.6299°N, 35.9937°W), garages, tent area, drill trench entrance are also shown. The EGRIP drill site is within 20 m of the drill trench entrance.

surface melting or internal melting in subsurface layers at the EGRIP site. However, this melting was not sufficient to disturb the stable water isotope and ion profiles. These ice layers appeared between summer 2011 and summer 2012 layers according to our dating. Surface snow/ice melting was observed over the Greenland Ice Sheet in July 2012 (Nghiem et al., 2012; Aoki et al., 2014). Meltwater should have also occurred at the EGRIP site in the summer of 2012, penetrated lower layers and refrozen in the layer between the summers of 2011 and 2012. Our dating explains this melting phenomenon well.

Surface mass balance for each year during the study period was calculated for each snow pit using annual layer thicknesses obtained from dating results and snow density profiles. An annual layer was defined as the layer between two consecutive summer layers. Winter layers were also determined using the minimum  $\delta^{18}\text{O}$  value within each annual layer. Each annual layer was subsequently divided into two halves and summer-to-winter and winter-to-summer snow depositions were calculated. Fig. 4 shows results from Pits 1 and 2. Surface mass balances in water equivalent (w.e.) obtained from Pit 1 varied between 58 and 202 mm w.e./yr, and that from Pit 2 varied between 126 and 188 mm w.e./yr. In both Pits 1 and 2, ice layers were found between the layers corresponding to the summers of 2011 and 2012. The snow melt that occurred in July 2012 should have redistributed water mass by refreezing of meltwater at the lower layers. The mean monthly isotopic compositions of precipitation at six sites on the Greenland coast show more enriched composition in June–August precipitation (data from IAEA/WMO, 2020). Annual summer peaks of  $\delta^{18}\text{O}$  and  $\delta\text{D}$  in the snow at the EGRIP site therefore seem to appear during these months. The melt event would have led to a decrease in the surface mass balance between summer 2012 and summer 2013 and an increase in the balance between summer 2011 and summer 2012.

Average surface mass balance between 2009 and 2016 was 145 mm w.e./yr in Pit 1 and 149 mm w.e./yr in Pit 2 (Nakazawa et al., submitted). Similar values of average surface mass balance were obtained from all pits (Komuro et al., 2020). While there was spatial and temporal variability in values of annual surface mass balance, there was little variability in the values of average surface mass balance over multiple years (ranging from 148 to 157 mm w.e./yr) and in the values of annual average surface mass balance of multiple pits (ranging from 134 to 157 mm w.e./yr). Spatial variability in surface mass balance is probably a result of post-depositional redistribution of snow caused by wind erosion and snowdrift. Our results suggest that surface mass balance in the EGRIP area was almost constant during 2009–2017 (Komuro et al., 2020), which is as much as 1.5 times higher than the average in 1607–2011 (Vallelonga et al., 2014). This substantial increase may be due to the recent warming in Greenland. We also found that seasonal snow depositions tended to be larger in the summer-to-winter period than in the winter-to-summer period (Table 2), the latter being about 85% of the former. Our results are opposite to those from the North Greenland Eemian Ice Drilling (NEEM) site (NEEM community members, 2013), which is located in Northwest Greenland (Kuramoto et al., 2011).

### 3. Flow properties of ice

Snow deposited onto the Greenland Ice Sheet is buried under

## Pit 1

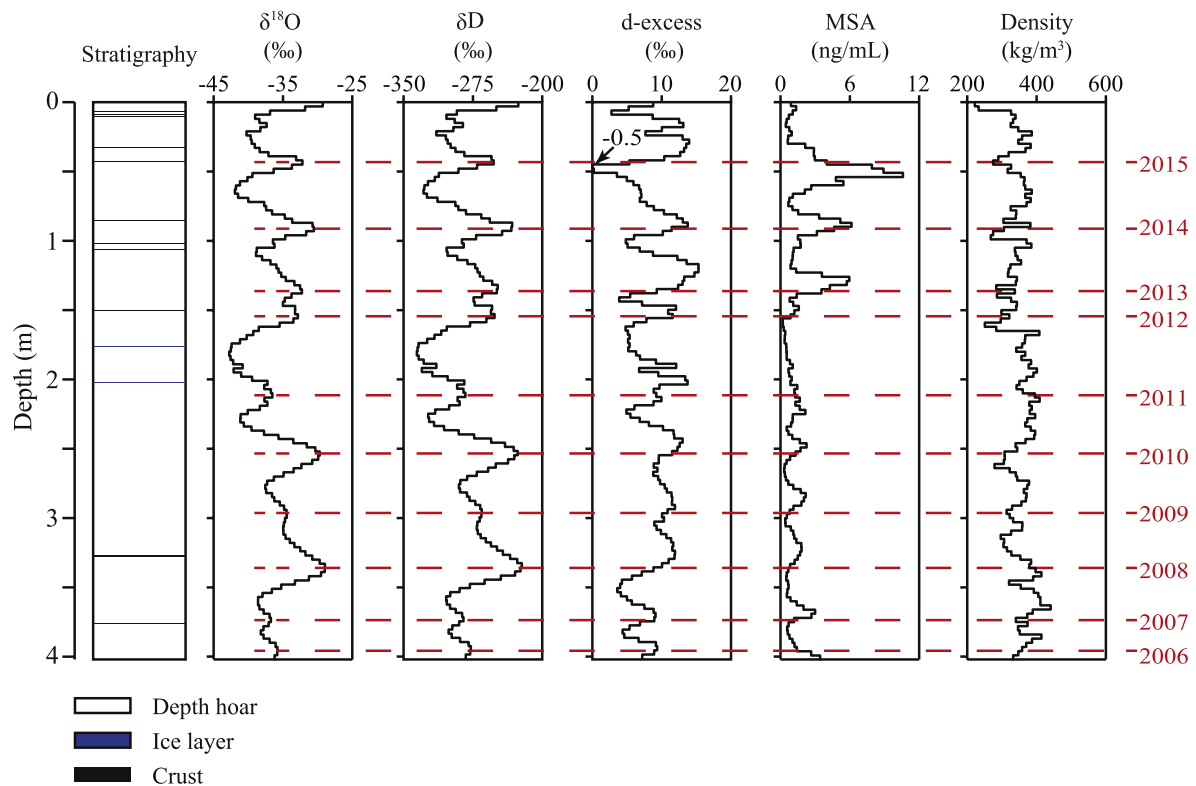


**Fig. 3.** Vertical profiles of stratigraphy,  $\delta^{18}\text{O}$ ,  $\delta\text{D}$ , d-excess, methanesulfonate (MSA) and density in Pit 1. Red dotted lines indicate annual summer layers. (For interpretation of the references to color in this figure legend, the reader is referred to the Web version of this article.)

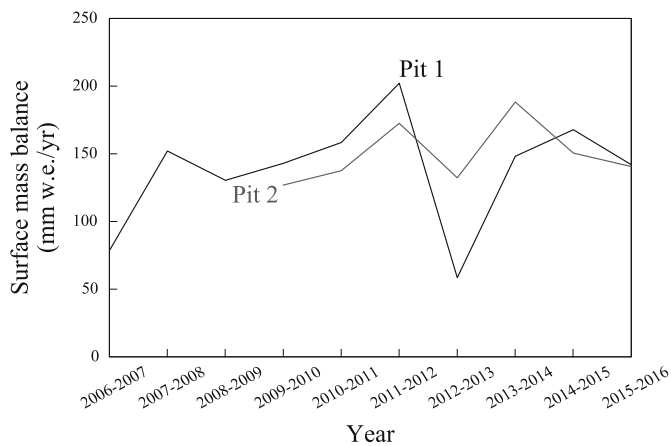


**Fig. 4.** Surface mass balances obtained from Pits 1 and 2.

subsequent layers of snow and eventually transforms into ice. Ice is exerted upon by gravity and is deformed. Ice deformation results in vertical and horizontal motion (i.e. flow) of the ice sheet. When ice reaches the ice sheet margin, it loses its mass either by melting or calving. Because calving strongly depends on ice flow velocity, accelerated ice sheet flow thus accelerates sea level rise (Van den Broeke et al., 2009). To make better projections of future sea level rise, we need to improve our understanding of the flow properties of ice. Crystal grain size, crystal orientation distribution and impurities in ice affect ice flow properties (Faria et al., 2014) and detailed mechanisms of ice flow still need to be ascertained.

Ice deformation has been traditionally described by Glen's flow law (Glen, 1955) or the following modified Glen's flow law (Goldsby and

Kohlstedt, 2001):

$$\dot{\epsilon} = A \frac{\sigma^n}{d^p} \exp\left(\frac{Q}{RT}\right) \quad (1)$$

where  $\dot{\epsilon}$  is strain rate,  $A$  is enhancement factor,  $\sigma$  is applied stress,  $d$  is average grain diameter,  $p$  is grain size parameter,  $R$  is the gas constant,  $n$  is the stress exponent, and  $T$  is absolute temperature. The value of  $n$  is usually set to 3 although a recent study reported that  $n = 4$  best fits observations of the Greenland Ice Sheet (Bons et al., 2018). Another study of laboratory experiments using fine-grained artificial ice without impurities indicated that  $n$  was close to 2 (Goldsby and Kohlstedt, 2001). To improve ice sheet flow models, it has become clear that, even as the mechanisms that give rise to different values of  $n$  remain poorly understood, the traditional flow law with  $n = 3$  needs to be reconsidered. To better understand ice flow properties, we carried out creep tests using artificial ice, separately identified the effects of microparticles and crystal grain size, and also determined  $n$  (Saruya et al., 2019).

We prepared powder snow by spraying pure water into liquid nitrogen. Some samples were prepared with water containing  $\text{SiO}_2$  (hereafter referred to as silica) particles of approximately 300 nm in diameter, and other samples were prepared without silica particles. Consolidated samples with and without silica particles were prepared by mechanically compressing the corresponding powder for 1 h at  $-10^\circ\text{C}$  and 70 MPa, and stacked alternately as shown in Fig. 5. The bulk sample in Fig. 5 was creep tested at  $-10^\circ\text{C}$  and 1 MPa. Layers containing silica deformed much more than pure ice layers during the test and their diameters became larger than those of the pure ice layers. This preliminary experiment highlights the effect of silica particles on ice deformation and demonstrates that ice sheet deformation can be modeled by deformation experiments using artificial ice samples with and without silica particles.

A similar creep test was performed using artificial ice containing

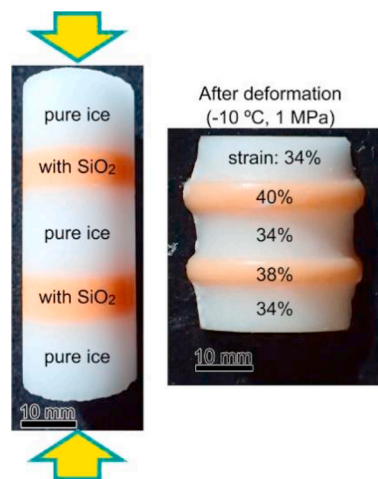


**Fig. 5.** Ice sample with (dark color) and without (white) silica particles before (left panel) and after (right panel) creep testing. (For interpretation of the references to color in this figure legend, the reader is referred to the Web version of this article.)

silica particles. The test was conducted at  $-20\text{ }^{\circ}\text{C}$ , which is a typical temperature in the Greenland Ice Sheet as observed from the borehole temperature profiles at GRIP and Dye 3 (Dahl-Jensen, 1998), and under 1 MPa, which was selected to achieve a relatively short test duration. For comparison, a pure ice sample was also prepared and tested under the same conditions and the results are shown in Fig. 6. We found that silica affected even the early stages of creep deformation. Over the entire range of measured strains, strain rate in pure ice was much lower than that of silica-dispersed ice, indicating that silica-dispersed ice deforms much more rapidly than pure ice, which agrees with the results shown in Fig. 5. In ice samples with large grain sizes, the strain rate usually decreases with strain at the beginning of a creep test as work hardening occurs because of interactions between dislocations (Wilson et al., 2014). Recovery or recrystallization usually follows, accumulated dislocations disappear, new strain-free grains nucleate, and strain rate decreases with strain at a slower rate. Minimum creep rate is reached when the effects of work hardening and recovery are in balance, after which strain rate starts to increase with strain (Wilson et al., 2014). However, our artificial ice samples exhibited a totally different behavior and we found no minimum creep rate or increase in strain rate in our experiments (Fig. 6).

Fig. 7 shows optical microscope images of microstructures of deformed samples at 10% strain. As a result of Zener drag—pinning of grain boundaries by silica particles (Humphreys and Hatherly, 2004)—

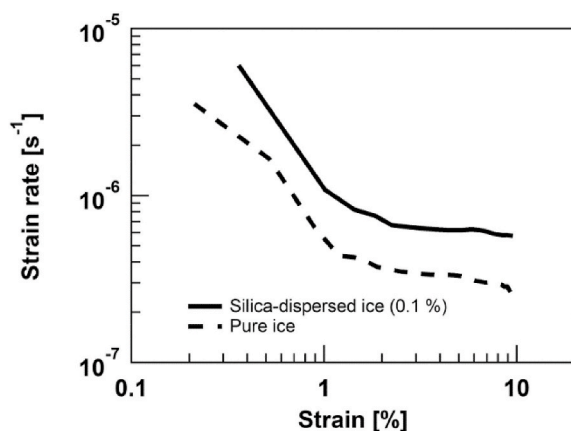


**Fig. 6.** Strain rate–strain diagrams calculated from creep curves derived under the conditions of  $-20\text{ }^{\circ}\text{C}$  and 1 MPa.

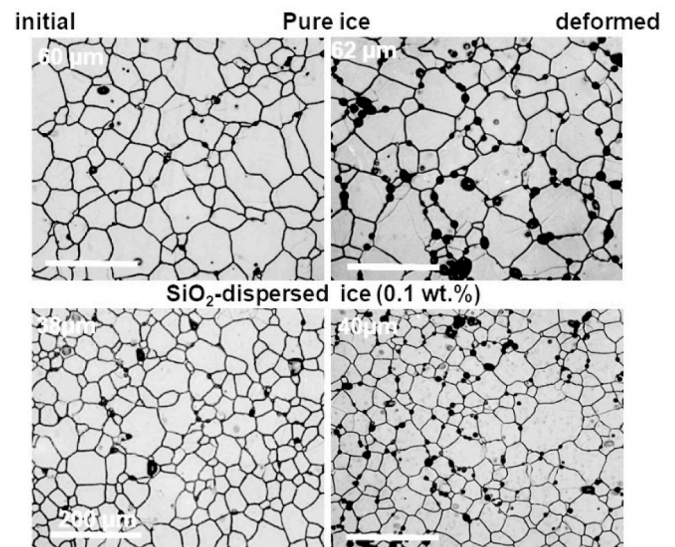


**Fig. 7.** Microstructural differences in artificial ice samples before and after achieving 10% strain under  $-20\text{ }^{\circ}\text{C}$  and 1 MPa.

the initial grain size in the silica-dispersed sample (mean diameter of approximately  $40\text{ }\mu\text{m}$ ) was smaller than that in the pure ice sample. When natural impurities transported by atmospheric circulation are deposited onto and incorporated into the Greenland Ice Sheet, such fine-grained ice layers can be generated locally as a result of seasonal variations and climate-dependent variations in impurity concentrations (Svensson et al., 2003). When ice core samples from Greenland are cut parallel to the core axis and observed perpendicular to the axis, so-called cloudy layers or bands are often visible (Faria et al., 2014). These layers were deposited mainly during glacial periods, and grain sizes are generally very small and concentrations of impurities are high (Faria et al., 2014).

To understand the creep mechanism of the silica-dispersed ice samples, we applied different stresses to the samples at constant temperature, measured strain rate, and derived values for the stress exponent  $n$ . We also derived the apparent activation energy  $Q$  by plotting strain rate as a function of the reciprocal of absolute temperature. We obtained  $n$  and  $Q$  values of 1.8–2.0 and 60–66 kJ/mol, respectively. These values are similar to those for fine-grained ice without microparticles reported by Goldsby and Kohlstedt (2001). By varying the compression conditions, we created artificial ice with larger grain sizes. This technique can be applied to both pure and silica-dispersed ice samples, and we obtained grain size diameters of approximately  $100\text{ }\mu\text{m}$  in pure ice. We also succeeded in preparing coarse-grained artificial ice by using a seed crystal of ice. We then evaluated the  $p$  value in the modified Glen flow law using results from the creep tests of fine- and coarse-grained artificial ice (Fig. 8). We found that  $p$  values converge towards the critical value of 1.4, implying that microparticles that are abundant in the deep parts of the ice sheet could influence ice sheet flow. Although the sizes of the ice grains in actual ice sheets are two orders of magnitude larger than in our artificial fine-grained ice, both are likely to experience similar deformation mechanisms because they deform under the situation in which the accumulation of dislocations is not saturated. More details are described by Saruya et al. (2019). Further analyses of the characteristics of microparticles in the Greenland Ice Sheet (e.g. size, shape, chemical composition) are needed to understand the mechanisms of ice sheet flow and predict future ice mass loss, which affects global climate and sea level. Ongoing studies on creep tests of the EGRIP core will contribute to the understanding of the effects of microparticles on ice deformation at the EGRIP site where horizontal flow velocity is high.

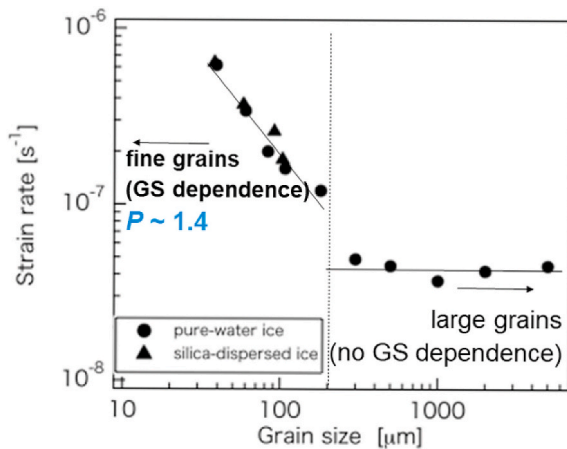


Fig. 8. Grain size (diameter) dependence of strain rate measured at  $-20^{\circ}\text{C}$  and 1 MPa.

#### 4. Numerical simulations: ice sheet modeling and GIA modeling

We carried out the following ice sheet and GIA modeling studies to improve future projections of sea level change and estimates of past ice sheet masses. For the ice flow, we used Glen's flow law (1) with the parameters by Greve (2019). In particular, we used a stress exponent of  $n = 3$  and grain size parameter  $p = 0$  to account for no dependence on grain size, and an additional flow enhancement factor  $E$  on the right-hand side.

In contrast to previous Greenlandic deep ice cores, the NEMM ice core was drilled in a region with significant shear deformation, which makes it useful for inferring ice-dynamical information. We analyzed NEMM borehole deformation data measured from borehole logging and calculated the flow enhancement factor as a function of the ice core's  $\delta^{18}\text{O}$  profile. We found a strong correlation down to millennial time scales (Dansgaard–Oeschger events), such that isotopically colder ice is softer and isotopically warmer ice is stiffer. For the isotopically coldest ice of the last glacial period, the enhancement factor reaches values up to  $\sim 40$ . We interpret this as a combined effect of impurities and flow-induced anisotropy (Greve et al., 2017, in preparation).

It is not clear at this stage whether these findings can be generalized

to larger parts of the ice sheet, or whether the dependence of ice deformability on climate varies strongly from place to place. For the purpose of large-scale modelling, we therefore mainly used a simpler, two-valued dependence, with  $E = 1$  for interglacial ice and  $E = 3$  for glacial ice. We implemented ice stream dynamics (Bernales et al., 2017) and a simple treatment of subglacial hydrology (Calov et al., 2018) in the ice sheet model Simulation CODE for POLythermal Ice Sheets (SICOPOLIS; [www.sicopolis.net](http://www.sicopolis.net)). We spun up SICOPOLIS and the Ice sheet model for Integrated Earth system Studies (ICES) to reproduce the present-day state of the Greenland Ice Sheet. For surface topography and velocity, there was good agreement between observed and simulated values (Goelzer et al., 2018, 2020; Greve, 2019). We used two warming scenarios based on Representative Concentration Pathway (RCP) 2.6 projections from climate models, which are in line with the commitments of the Paris Agreement, to force SICOPOLIS and the Ice Sheet System Model (ISSM; [issm.jpl.nasa.gov](http://issm.jpl.nasa.gov)). The results show that the mass loss of the Greenland Ice Sheet is projected to be 62–88 mm sea level equivalent for the period of 1990–2300 (Rückamp et al., 2019). As our contribution to ISMIP6, we used the latest version of the SICOPOLIS model (version 5.1 that includes ice stream dynamics, subglacial hydrology and a depth-dependent flow enhancement factor; Greve and SICOPOLIS Developer Team, 2019), forced by output from a representative subset of CMIP5 and CMIP6 global climate models, to project ice sheet changes and sea level rise contributions over the 21st century (Goelzer et al., 2020; Greve et al., 2020). The results are shown in Fig. 9. The simulated sea level contribution for 1990–2100 is  $133.0 \pm 40.7$  mm (mean  $\pm 1$ -sigma uncertainty) for the RCP8.5/SSP5-8.5 pathway that represents “business as usual”, and it is  $48.6 \pm 6.2$  mm for the RCP2.6/SSP1-2.6 pathway that represents substantial emissions reductions. The large difference between the results for the two pathways highlights the importance of efficient climate change mitigation for limiting sea level rise.

We developed a GIA model that takes into account a realistic viscosity structure of the lower mantle, reconstructed ice sheet volume at the Last Glacial Maximum (LGM) and calculated the change of degree-two harmonics of the Earth's geopotential (Nakada et al., 2016). We examined variations of total meltwater volume during the last deglaciation and determined the contributions of different continental ice sheets, including the Greenland Ice Sheet. We found that the lower degree geopotential data were critical in the estimation of both global ice volume at the LGM and lower mantle viscosity structure. Our results

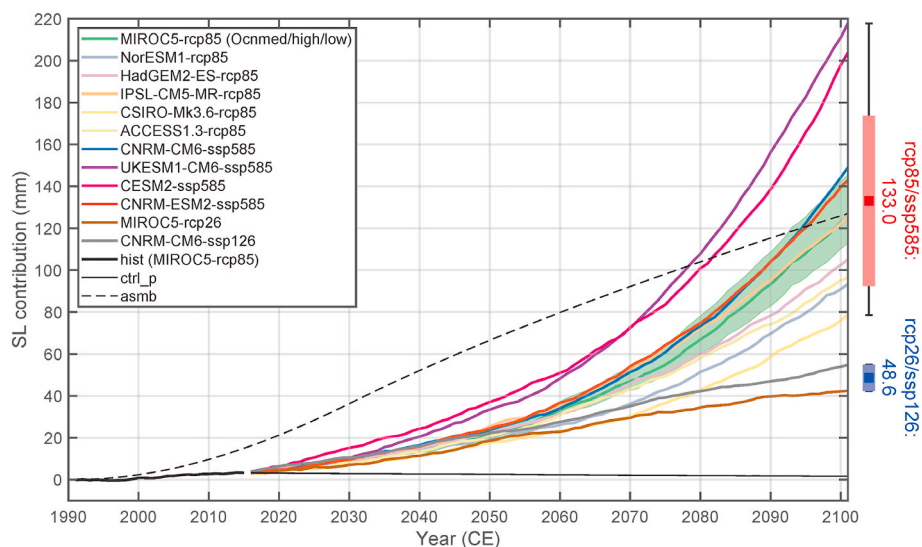


Fig. 9. Contribution to sea level (SL) rise due to ice mass loss from the Greenland Ice Sheet simulated by SICOPOLIS as part of ISMIP6. hist is the historical run, ctrl\_p is the constant-climate control run, and asmb is a schematic surface-mass-balance-anomaly experiment (Goelzer et al., 2018). All other experiments are driven by atmospheric and oceanic forcings derived from global climate models for either RCP8.5/SSP5-8.5 or RCP2.6/SSP1-2.6 pathways.

provide valuable insight to understand past variabilities of the Greenland Ice Sheet, which is essential for constraining ice sheet models.

## 5. Environmental changes associated with past climate changes

For better projections of future environmental changes due to global warming, we need to evaluate the impacts of past environmental changes associated with warming. To understand the impacts of global warming on terrestrial and marine environments in the middle to high latitudes of the Northern Hemisphere, we used three Greenland ice cores covering different time periods. All of the cores include past warm periods although on different time scales ranging from 350 to 130,000 years.

Variations in terrestrial environments over the past 130,000 years were reconstructed using ion data from the NEEM ice core (Schüpbach et al., 2018). Compared with the present day, temperature during the early Holocene was 2–3 °C higher and temperature during the last interglacial period was 8 °C higher. However, North American terrestrial vegetation varied little between the two periods. Emissions of mineral dust from East Asia during the last interglacial period were only moderately (30%) higher than those of the early Holocene. A temperature that is 8 °C higher than present day in Greenland is similar to the polar amplification signal forecasted for a global warming of 1.5–2 °C (Otto-Bliesner et al., 2013). Therefore, these results suggest that if global mean temperature increase can be kept within 1.5–2 °C above pre-industrial levels, there is likely to be little change in terrestrial environments in the middle to high latitudes in the Northern Hemisphere.

Sea ice extent in the Canadian Arctic over the past 110,000 years was reconstructed using the bromine data from the NEEM ice core (Spolaor et al., 2016). Results show that multi-year ice in the Canadian Arctic increased during cold stadials of the last glacial period, while the extent of first-year ice reached its maximum during the early Holocene, suggesting that multi-year ice in the Arctic Ocean would decrease under future warming.

In collaboration with Research Theme 3 of the ArCS project, black carbon (BC) variations over the past 350 years were reconstructed from an ice core drilled at the SIGMA-D site in Northwest Greenland (Matoba et al., 2015). The Wide-Range Single Particle Soot Photometer (SP2) developed at the University of Tokyo (Mori et al., 2016)—modified from the SP2 of Droplet Measurement Technologies (Longmont, CO., U.S.A.)—and the Continuous Flow Analysis System (Dallmayr et al., 2016) developed at the National Institute of Polar Research were used to produce a high-resolution and high-accuracy reconstruction of BC concentrations and size distributions. Anthropogenic BC increased during the first half of the 20th century and annual peaks of BC shifted from summer to winter because of anthropogenic input. Sporadic BC peaks in summers were likely results of boreal forest fires in North America and/or Siberia (Zennaro et al., 2014). Although Greenland has undergone recent rapid warming (Kobashi et al., 2011), we found no evidence of increased boreal forest fires over the last 20 years. However, for the present warm period and the warm period of 1920–1940, we found that mineral dust at the SIGMA-D site largely originated from high-latitude sources including local sources in Greenland while low or mid-latitude sources were dominant during the cold periods of the 20th century. These results suggest that high-latitude dust sources would become more important under global warming.

In collaboration with international EGRIP members and Research Theme 3 of the ArCS project, we analyzed BC in the EGRIP core. The EGRIP core has been dated preliminarily by relating acidity peaks in the core to volcanic events (Mojtabavi et al., in review, 2019). Preliminary BC concentration data over the past 200 years appear to show seasonal variations and increases during the first half of the 20th century. We expect that further detailed dating and BC analysis back to the early Holocene warm period will reveal changes in boreal forest fires in association with past warming.

## 6. Summary and future prospects

We carried out snow pit studies to assess the spatial variability of recent surface mass balance in the area around the EGRIP deep drilling site in East Greenland, where direct observations are scarce (Nakazawa et al., submitted; Komuro et al., 2020). While spatial and temporal variability of annual surface mass balance values are likely due to effects of wind scouring, there was little variability in the average surface mass balance values over multiple years and in multiple pits. This confirms the representativity of our pit data for the EGRIP area. The surface mass balance in the EGRIP area was surprisingly constant during 2009–2017. However, compared with the 1607–2011 average (Vallelonga et al., 2014), we found a substantial increase in recent surface mass balance by as much as 50%, which is likely associated with recent warming. We must therefore reconstruct annual surface mass balances over the past 400 years and investigate the detailed mechanisms of their recent increase. Our new data can serve as ground truth data for satellite observations and contribute to validate climate models, which are essential to improve projections of future changes in mass balance of the Greenland Ice Sheet and in global climate and the environment.

The NEEM borehole data suggest that impurities strongly enhance ice deformation (see Section 4). In ice sheets, however, smaller grain size is usually associated with higher microparticle concentration (Faria et al., 2014), which makes it difficult to separate the effects of grain size and microparticles. Using artificial ice with grain sizes and microparticle concentrations that were independently regulated, we investigated the effects of microparticles and grain sizes separately (Saruya et al., 2019). We found that grain size, not microparticle concentration, is a dominant factor regulating the deformation rate of ice. To apply our new flow law, which takes into account effects of grain size and microparticles, to the Greenland Ice sheet, we still need to perform creep tests using ice samples from NEEM and EGRIP ice cores because microparticle concentrations were much higher and grain sizes were much smaller in our artificial ice samples, compared with those in these ice cores. The EGRIP ice core will provide unique information on ice dynamics because the drill site is located in an area with considerably high horizontal flow velocity compared to previous deep drilling sites.

Analysis of NEEM borehole deformation data revealed a strong correlation between climatic states and ice deformability down to the time scales of millennial-scale warming events. For the coldest ice of the last glacial period, the flow enhancement factor reaches values up to ~40, which is substantially larger than previously thought. We will need to confirm that this finding can be generalized to larger parts of the ice sheet and incorporate it into large scale ice sheet modeling. Within the 5-year ArCS project, we mainly used simpler ice-sheet models. However, by taking into account ice stream dynamics and subglacial hydrology, we improved our ice sheet models and reproduced the present-day state of the Greenland Ice Sheet. We also performed new projections of the future contribution of the Greenland ice sheet to sea level rise by improving the ice sheet models and using the latest results from climate models. As a next step, we will continue observations of the EGRIP borehole deformation after completion of the deep ice drilling so that we can obtain more spatial information on the correlation between climatic states and ice deformability. We need to perform longer-term future climate/ice sheet change simulations (e.g. until the year 3000). Furthermore, we need to incorporate the results from creep tests and GIA modeling into ice sheet modeling.

We reconstructed the past environmental changes during the past warming periods on different time scales, mainly focusing on terrestrial and sea-ice conditions. Ongoing high-resolution analyses on the EGRIP core, the first deep ice core in East Greenland, will provide new insight into the mechanisms and impacts of environmental changes during the early Holocene, which was 2–3 °C warmer than today (Schüpbach et al., 2018).

The studies summarized above were carried out rather independently. In the future, we will need to integrate the results obtained from

each project in ice sheet and climate modeling.

### Declaration of competing interest

The authors declare that they have no known competing financial interests or personal relationships that could have appeared to influence the work reported in this paper.

### Acknowledgments

Funding: The research was supported by the Arctic Challenge for Sustainability (ArCS) Project (Program Grant Number JPMXD130000000), JSPS KAKENHI (grant numbers JP23221004, JP16H01772, JP16H02224, JP16K01229, JP17H02957, JP17H06104, JP17H06323, JP18H04140), the Environment Research and Technology Development Funds (JPMEERF20172003 and JPMEERF20202003) of the Environmental Restoration and Conservation Agency of Japan, National Institute of Polar Research (Project Research KP305), and the Joint Research Program of the Japan Arctic Research Network Center in 2017.

We would like to thank the EGRIP members who supported the ice coring and pit observations at EGRIP. EGRIP is directed and organized by the Center of Ice and Climate at the Niels Bohr Institute and US NSF, Office of Polar Programs. It is supported by funding agencies and institutions in Denmark (A. P. Møller Foundation, UCPH), US (US NSF, Office of Polar Programs), Germany (AWI), Japan (National Institute of Polar Research and ArCS), Norway (BFS), Switzerland (SNF), France (IPEV, IGE) and China (CAS). We are also grateful to the laboratory technicians at the National Institute of Polar Research who analyzed the snow-pit and ice-core samples.

We thank the Climate and Cryosphere (CliC) project for providing support for ISMIP6 through sponsoring of workshops, hosting the ISMIP6 website and wiki and promoting ISMIP6. We acknowledge the World Climate Research Programme and its Working Group on Coupled Modeling for coordinating and promoting CMIP5 and CMIP6. We thank the climate modelling groups for producing and making available their model output, the Earth System Grid Federation (ESGF), for archiving the CMIP data and providing access, the University at Buffalo for ISMIP6 data distribution and upload, and the multiple funding agencies who support CMIP5, CMIP6 and the ESGF. We thank the ISMIP6 model selection group and ISMIP6 dataset preparation group for their continuous engagement in defining ISMIP6. This is ISMIP6 contribution No. 20.

### References

AMAP, 2017. Snow, Water, Ice and Permafrost in the Arctic (SWIPA) 2017. Arctic Monitoring and Assessment Programme (AMAP), Oslo, Norway, p. 269.

Aoki, T., Matoba, S., Uetake, J., Takeuchi, N., Motoyama, H., 2014. Field activities of the “snow impurity and glacial microbe effects on abrupt warming in the arctic” (SIGMA) project in Greenland in 2011–2013. *Bull. Glaciol. Res.* 32, 3–20. <https://doi.org/10.5331/bgr.32.3>.

Bernales, J., Rogozhina, I., Greve, R., Thomas, M., 2017. Comparison of hybrid schemes for the combination of shallow approximations in numerical simulations of the Antarctic Ice Sheet. *Cryosphere* 11, 247–265. <https://doi.org/10.5194/tc-11-247-2017>.

Bons, P.D., Kleiner, T., Llorens, M.-G., Prior, D.J., Sachau, T., Weikusat, I., Jansen, D., 2018. Greenland Ice Sheet: higher nonlinearity of ice flow significantly reduces estimated basal motion. *Geophys. Res. Lett.* 45, 6542–6548. <https://doi.org/10.1029/2018GL078356>.

Calov, R., Beyer, S., Greve, R., Beckmann, J., Willeit, M., Kleiner, T., Rückkamp, M., Humbert, A., Ganopolski, A., 2018. Simulation of the future sea level contribution of Greenland with a new glacial system model. *Cryosphere* 12, 3097–3121. <https://doi.org/10.5194/tc-12-3097-2018>.

Dahl-Jensen, D., 1998. Past temperatures directly from the Greenland ice sheet. *Science* 282, 268–271. <https://doi.org/10.1126/science.282.5387.268>.

Dallmayer, R., Goto-Azuma, K., Kjær, H., Azuma, N., Takata, M., Schüpbach, S., Hirabayashi, M., 2016. A high-resolution Continuous Flow Analysis System for polar ice cores. *Bull. Glaciol. Res.* 34, 11–20. <https://doi.org/10.5331/bgr.16R03>.

Fahnestock, M.A., Bindschadler, R., Kwok, R., Jezek, K., 1993. Greenland ice sheet surface properties and ice dynamics from ERS-1 SAR imagery. *Science* 262, 1530–1534. <https://doi.org/10.1126/science.262.5139.1530>.

Fahnestock, M.A., Joughin, I., Scambos, T.A., Kwok, R., Krabill, W.B., Gogineni, S., 2001. Ice-stream-related patterns of ice flow in the interior of northeast Greenland. *J. Geophys. Res.* 106, 34035–34045. <https://doi.org/10.1029/2001JD900194>.

Faria, S.H., Weikusat, I., Azuma, N., 2014. The microstructure of polar ice. Part I: highlights from ice core research. *J. Struct. Geol.* 61, 2–20. <https://doi.org/10.1016/j.jsg.2013.09.010>.

Glen, J.W., 1955. The creep of polycrystalline ice. *Proc. R. Soc. London Ser. A* 228, 519–538. <https://doi.org/10.1098/rspa.1955.0066>.

Goelzer, H., Nowicki, S., Edwards, T., Beckley, M., Abe-Ouchi, A., Aschwanden, A., Barthel, R., Gagliardini, O., Gillet-Chaulet, F., Gollledge, N.R., Gregory, J., Greve, R., Humbert, A., Huybrechts, P., Kennedy, J.H., Larour, E., Lipscomb, W.H., Le clec’h, S., Lee, V., Morlighem, M., Pattyn, F., Payne, A.J., Rodehacke, C., Rückkamp, M., Saito, F., Schlegel, N., Seroussi, H., Shepherd, A., Sun, S., van de Wal, R., Ziemann, F.A., 2018. Design and results of the ice sheet model initialisation experiments initMIP-Greenland: an ISMIP6 intercomparison. *Cryosphere* 12, 1433–1460. <https://doi.org/10.5194/tc-12-1433-2018>.

Goelzer, H., Nowicki, S., Payne, A., Larour, E., Seroussi, H., Lipscomb, W.H., Gregory, J., Abe-Ouchi, A., Shepherd, A., Simon, E., Agosta, C., Alexander, P., Aschwanden, A., Barthel, R., Calov, R., Chambers, C., Choi, Y., Cuzzone, J., Dumas, C., Edwards, T., Felikson, D., Fettweis, X., Gollledge, N.R., Greve, R., Humbert, A., Huybrechts, P., Le clec’h, S., Lee, V., Leguy, G., Little, C., Lowry, D.P., Morlighem, M., Nias, I., Quiquet, A., Rückkamp, M., Schlegel, N.-J., Slater, D., Smith, R., Straneo, F., Tarasov, L., van de Wal, R., van den Broeke, M., 2020. The future sea-level contribution of the Greenland ice sheet: a multi-model ensemble study of ISMIP6. *Cryosphere* 14. <https://doi.org/10.5194/tc-14-xxxx-2020>. In press.

Goldsbury, D.L., Kohlstedt, D.L., 2001. Superplastic deformation of ice: experimental observations. *J. Geophys. Res.* 106, 11017–11030. <https://doi.org/10.1029/2000JB900336>.

Greve, R., 2019. Geothermal heat flux distribution for the Greenland ice sheet, derived by combining a global representation and information from deep ice cores. *Polar Data J.* 3, 22–36. <https://doi.org/10.20575/00000006>.

Greve, R., Chambers, C., Calov, R., 2020. ISMIP6 future projections for the Greenland ice sheet with the model SICOPOLIS. Zenodo (Technical report). <https://doi.org/10.5281/zenodo.3971251>.

Greve, R., Dahl-Jensen, D., Hvidberg, C.S., 2017. Connection between Climatic State and Ice Softness Derived from Deformation Measurements of the Greenlandic NEMM Borehole. Abstract C44A-02 presented at 2017 Fall Meeting, AGU, New Orleans, USA, 11–15 Dec.

Greve, R., SICOPOLIS Developer Team, 2019. SICOPOLIS v5.1. Zenodo. <https://doi.org/10.5281/zenodo.3727511>.

Humphreys, F.J., Hatherly, M., 2004. Recrystallization and Related Annealing Phenomena, second ed. Elsevier, Amsterdam.

IAEA/WMO, 2020. The Global Network of Isotopes in Precipitation. The GNIP Database. IAEA/WMO, Vienna. <https://nucleus.iaea.org/wiser>.

IPCC, 2013. Climate Change 2013: The Physical Science Basis. Contribution of Working Group I to the Fifth Assessment Report of the Intergovernmental Panel on Climate Change. Cambridge University Press, Cambridge, United Kingdom and New York, NY, USA, p. 1535.

Jaffrezo, J.L., Davidson, C.I., Legrand, M., Dibb, J.E., 1994. Sulfate and MSA in the air and snow on the Greenland ice sheet. *J. Geophys. Res.* 99, 1241–1253. <https://doi.org/10.1029/93JD02913>.

Johnsen, S.J., Dansgaard, W., White, J.W.C., 1989. The origin of Arctic precipitation under present and glacial conditions. *Tellus B* 41, 452–468. <https://doi.org/10.1111/j.1600-0889.1989.tb00321.x>.

Joughin, I., Fahnestock, M., MacAyeal, B., Bamber, J.L., Gogineni, P., 2001. Observation and analysis of ice flow in the largest Greenland ice stream. *J. Geophys. Res.* 106, 34021–34034. <https://doi.org/10.1029/2001jd900087>.

Kobashi, T., Kawamura, K., Severinghaus, J.P., Barnola, J.-M., Nakaegawa, T., Vinther, B.M., Johnsen, S.J., Box, J.E., 2011. High variability of Greenland surface temperature over the past 4000 years estimated from trapped air in an ice core. *Geophys. Res. Lett.* 38, L21501 doi: 10.29/2011gl049444.

Komuro, Y., Nakazawa, F., Hirabayashi, M., Goto-Azuma, K., Nagatsuka, N., Shigeyama, W., Matoba, S., Homma, T., Steffensen, J.P., Dahl-Jensen, D., in press, 2020. Temporal and spatial variabilities in surface mass balance at the EGRIP site, Greenland from 2009 to 2017. *Polar Sci.*

Kuramoto, T., Goto-Azuma, K., Hirabayashi, M., Miyake, T., Motoyama, H., Dahl-Jensen, D., Steffensen, J.P., 2011. Seasonal variations of snow chemistry at NEMM, Greenland. *Ann. Glaciol.* 52 (58), 93–200. <https://doi.org/10.3189/172756411797252365>.

Li, S.-M., Barrie, L.A., Talbot, R.W., Hariss, R.C., Davidson, C.I., Jaffrezo, J.L., 1993. Seasonal and geographic variations of methanesulfonic acid in the Arctic troposphere. *Atmos. Environ.* 27A, 3011–3024. [https://doi.org/10.1016/0960-1686\(93\)90333-T](https://doi.org/10.1016/0960-1686(93)90333-T).

Matoba, S., Motoyama, H., Fujita, K., Yamasaki, T., Minowa, M., Onuma, Y., Komuro, Y., Aoki, T., Yamaguchi, S., Sugiyama, S., Enomoto, H., 2015. Glaciological and meteorological observations at the SIGMA-D site, northwestern Greenland Ice Sheet. *Bull. Glaciol. Res.* 33, 7–14. <https://doi.org/10.5331/bgr.33.7>.

Mojtabavi, S., Wilhelmus, F., Cook, E., Davies, S., Sennelager, G., Jensen, M.S., Dahl-Jensen, D., Svensson, A., Vinther, B., Kipfstuhl, S., Jones, G., Karlsson, N.B., Faria, S.H., Gkinis, V., Kjær, H., Erhardt, T., Berben, S., Nisancioglu, K., Rasmussen, S.O., 2019. A first chronology for the East Greenland Ice-core Project (EastGRIP) over the Holocene and last glacial termination. submitted for publication *Clim. Past Discuss.* <https://doi.org/10.5194/cp-2019-143>.

Mori, T., Moteki, N., Ohata, S., Koike, M., Goto-Azuma, K., Miyazaki, Y., Kondo, Y., 2016. Improved technique for measuring the size distribution of black carbon particles in liquid water. *Aerosol Sci. Technol.* 50, 242–254. <https://doi.org/10.1080/02786826.2016.1147644>.

Nakada, M., Okuno, J., Yokoyama, Y., 2016. Total meltwater volume since the Last Glacial Maximum and viscosity structure of Earth’s mantle inferred from relative sea

- level changes at Barbados and Bonaparte Gulf and GIA-induced J2. *Geophys. J. Int.* 204, 1237–1253. <https://doi.org/10.1093/gji/ggy520>.
- Nakazawa, F., Nagatsuka, N., Hirabayashi, M., Goto-Azuma, K., Steffensen, J.P., Dahl-Jensen, D., submitted. Variation in recent annual snow deposition and seasonality of snow chemistry at the East Greenland Ice Core Project (EGRIP) camp, Greenland. *Polar Sci.*
- NEEM community members, 2013. Eemian interglacial reconstructed from a Greenland folded ice core. *Nature* 493, 489–494. <https://doi.org/10.1038/nature11789>.
- Nghiem, S.V., Hall, D.K., Mote, T.L., Tedesco, M., Albert, M.R., Keegan, K., Shuman, C.A., DiGirolamo, N.E., Neumann, G., 2012. The extreme melt across the Greenland ice sheet in 2012. *Geophys. Res. Lett.* 39, L20502. <https://doi.org/10.1029/2012GL053611>.
- Nowicki, S., Goelzer, H., Seroussi, H., Payne, A.J., Lipscomb, W.H., Abe-Ouchi, A., Agosta, C., Alexander, P., Asay-Davis, X.S., Barthel, A., Bracegirdle, T.J., Cullather, R., Felikson, D., Fettweis, X., Gregory, J.M., Hatterman, T., Jourdain, N.C., Kuipers Munneke, P., Larour, E., Little, C.M., Morlighem, M., Nias, I., Shepherd, A., Simon, E., Slater, D., Smith, R.S., Straneo, F., Trusel, L.D., van den Broeke, M.R., van de Wal, R., 2020. Experimental protocol for sea level projections from ISMIP6 stand-alone ice sheet models. *Cryosphere* 14, 2331–2368. <https://doi.org/10.5194/tc-14-2331-2020>.
- Otto-Bliesner, B.L., Rosenbloom, N., Stone, E.J., McKay, N.P., Lunt, D.J., Brady, E.C., Overpeck, J.T., 2013. How warm was the last interglacial? New model–data comparisons. *Philos. Trans. R. Soc. A* 371, 20130097. <https://doi.org/10.1098/rsta.2013.0097>.
- Rignot, E., Velicogna, I., van den Broeke, M.R., Monaghan, A., Lenaerts, J.T.M., 2011. Acceleration of the contribution of the Greenland and Antarctic ice sheets to sea level rise. *Geophys. Res. Lett.* 38, L05503. <https://doi.org/10.1029/2011GL046583>.
- Rückamp, M., Greve, R., Humbert, A., 2019. Comparative simulations of the evolution of the Greenland ice sheet under simplified Paris Agreement scenarios with the models SICOPOLIS and ISSM. *Polar Sci.* 21, 14–25. <https://doi.org/10.1016/j.polar.2018.12.003>.
- Saruya, T., Nakajima, N., Takata, M., Homma, T., Azuma, N., Goto-Azuma, K., 2019. Effects of microparticles on deformation and microstructural evolution of fine-grained ice. *J. Glaciol.* 65, 531–541. <https://doi.org/10.1017/jog.2019.29>.
- Schüpbach, S., Fischer, H., Bigler, M., Erhardt, T., Gfeller, G., Leuenberger, D., Mini, O., Mulvaney, O., Abram, N.J., Fleet, L., Frey, M.M., Thomas, E., Svensson, A., Dahl-Jensen, D., Kettner, E., Kjaer, H., Seierstad, I., Steffensen, J.P., Rasmussen, S.O., Vallenga, P., Winstrup, M., Wegner, A., Twarloh, B., Wolff, K., Schmidt, K., Goto-Azuma, K., Kuramoto, K., Hirabayashi, M., Uetake, J., Zheng, J., Bourgeois, J., Fisher, D., Zhiheng, D., Xiao, C., Legrand, M., Spolaor, A., Gabrieli, J., Barbante, C., Kang, J.-H., Hur, S.D., Hong, S.B., Hwang, H.J., Hong, S., Hansson, M., Ilzuka, Y., Oyabu, I., Muscheler, R., Adolphi, F., Maselli, O., McConnell, J., Wolff, E.W., 2018. Greenland records of aerosol source and atmospheric lifetime changes from the Eemian to the Holocene. *Nat. Commun.* 9, 1476. <https://doi.org/10.1038/s41467-018-03924-3>.
- Spolaor, A., Vallenga, P., Turetta, C., Maffezzoli, N., Cozzi, G., Gabrieli, J., Barbante, C., Goto-Azuma, K., Saiz-Lopez, A., Cuevas, C.A., Dahl-Jensen, D., 2016. Canadian Arctic sea ice reconstructed from bromine in the Greenland NEEM ice core. *Sci. Rep.* 6, 33925. <https://doi.org/10.1038/srep33925>.
- Sugiyama, S., Kanna, N., Sakakibara, D., Ando, T., Asaji, I., Kondo, K., Wang, Y., Fujishi, Y., Fukumoto, S., Podolskiy, E., Fukamachi, Y., Takahashi, M., Matoba, S., Ilzuka, Y., Greve, R., Furuya, M., Tateyama, K., Watanabe, T., Yamasaki, S., Yamaguchi, A., Nishizawa, B., Matsuno, K., Nomura, D., Sakuragi, Y., Matsumura, Y., Ohashi, Y., Aoki, T., Niwano, M., Hayashi, N., Minowa, M., Jouvet, G., Funk, M., Bjørk, A.A., submitted. Rapidly changing glaciers, ocean and coastal environments, and their impact on human society in the Qaanaaq region, northwestern Greenland. *Polar Sci.*
- Svensson, A., Baadsager, P., Persson, A., Hvidberg, C.S., Siggaard-Andersen, M.L., 2003. Seasonal variability in ice crystal properties at NorthGRIP: a case study around 301 m depth. *Ann. Glaciol.* 37, 119–122. <https://doi.org/10.3189/172756403781815582>.
- The IMBIE Team, 2020. Mass balance of the Greenland ice sheet from 1992 to 2018. *Nature* 579, 233–239. <https://doi.org/10.1038/s41586-019-1855-2>.
- Vallenga, P., Christianson, K., Alley, R.B., Anandakrishnan, S., Christian, J.E.M., Dahl-Jensen, D., Gkinis, V., Holme, C., Jacobel, R.W., Karlsson, N.B., Keisling, B.A., Kipfstuhl, S., Kjær, H.A., Kristensen, M.E.L., Muto, A., Peters, L.E., Popp, T., Riverman, K.L., Svensson, A.M., Tibuleac, C., Vinther, B.M., Weng, Y., Winstrup, M., 2014. Initial results from geophysical surveys and shallow coring of the Northeast Greenland Ice Stream (NEGIS). *Cryosphere* 8, 1275–1287. <https://doi.org/10.5194/tc-8-1275-2014>.
- Van den Broeke, M., Bamber, J., Ettema, J., Rignot, E., Schrama, E., van de Berg, W.J., van Meijgaard, E., Velicogna, I., Wouters, B., 2009. Partitioning recent Greenland mass loss. *Science* 326, 984–986. <https://doi.org/10.1126/science.1178176>.
- Wilson, C.J.L., Peternell, M., Piazzolo, S., Luzin, V., 2014. Microstructure and fabric development in ice: lessons learned from in situ experiments and implications for understanding rock evolution. *J. Struct. Geol.* 61, 50–77. <https://doi.org/10.1016/j.jsg.2013.05.006>.
- Zennaro, P., Kehrwald, N., McConnell, J.R., Schüpbach, S., Maselli, O.J., Marlon, J., Vallenga, P., Leuenberger, D., Zangrando, R., Spolaor, A., Borrotti, M., Barbaro, E., Gambaro, A., Barbante, C., 2014. Fire in ice: two millennia of boreal forest fire history from the Greenland NEEM ice core. *Clim. Past* 10, 1905–1924. <https://doi.org/10.5194/cp-10-1905-2014>.